Accepted Manuscript

Stereology shows that damaged liver recovers after protein refeeding

Silvio Pires Gomes, Andréa Almeida Pinto da Silva, Amanda Rabello Crisma, Primavera Borelli, Francisco Javier Hernandez-Blazquez, Mariana P. de Melo, Barbara Bacci, Andrzej Loesch, A. Augusto Coppi

PII: S0899-9007(17)30042-4

DOI: 10.1016/j.nut.2017.02.010

Reference: NUT 9926

To appear in: *Nutrition*

Received Date: 3 August 2016

Revised Date: 4 January 2017

Accepted Date: 18 February 2017

Please cite this article as: Gomes SP, da Silva AAP, Crisma AR, Borelli P, Hernandez-Blazquez FJ, de Melo MP, Bacci B, Loesch A, Coppi AA, Stereology shows that damaged liver recovers after protein refeeding, *Nutrition* (2017), doi: 10.1016/j.nut.2017.02.010.

Stereology shows that damaged liver recovers after protein refeeding

Silvio Pires Gomes[1], Andréa Almeida Pinto da Silva[1], Amanda Rabello Crisma[2], Primavera Borelli[2], Francisco Javier Hernandez-Blazquez[1], Mariana P de Melo[3], Barbara Bacci[5], Andrzej Loesch[4], A. Augusto Coppi[5*]

[1]Laboratory of Stochastic Stereology and Chemical Anatomy (LSSCA), Department of Surgery, College of Veterinary Medicine and Animal Science, University of São Paulo (USP), São Paulo, Brazil,

[2]Laboratory of Haematology, Department of Clinical and Toxicological Analyses, Faculty of Pharmaceutical Sciences, University of São Paulo (USP), São Paulo, Brazil,

[3]Department of Basic and Environmental Sciences, Engineering School of Lorena, University of Sao Paulo (USP), Lorena, Brazil,

[4]Division of Medicine, University College London School of Life and Medical Sciences, Royal Free Campus, UK.

[5]School of Veterinary Medicine, Faculty of Health and Medical Sciences, University of Surrey, Guildford, Surrey, United Kingdom.

[*]**Corresponding author:** Dr Augusto Coppi. School of Veterinary Medicine, Faculty of Health and Medical Sciences, University of Surrey, Guildford, Surrey, GU2 7XH, United Kingdom. Email: a.coppi@surrey.ac.uk

Abstract

Objective: To investigate the putative effects of a low-protein diet on the 3D structure of hepatocytes and whether this scenario could be reversed by restoring the adequate levels of protein in the diet.

Methods: Using design-based stereology the total number and volume of hepatocytes were estimated in the liver of mice in healthy and altered (by protein malnutrition) conditions and after protein renutrition.

Results: This study has shown a 65% decrease in the liver volume (3,302 mm^3 for the control for undernourished vs 1,141 mm^3 for the undernourished group) accompanied by a 46% reduction in the hepatocyte volume (8,223 μm^3 for the control for undernourished vs 4,475 μm^3 for the undernourished group) and a 90% increase in the total number of binucleate hepatocytes. (1,549,393 for the control for undernourished vs 2,941,353 for the undernourished group). Reinstating a normoproteinic diet (12% casein) proved to be effective in restoring the size of hepatocytes, led to an 85% increase in the total number of uninucleate hepatocytes (15,988,560 for the undernourished vs 29,600,520 for the renourished group), and partially reversed the liver atrophy.

Conclusions: Awareness of these data will add to our better morphological understanding of malnutrition-induced hepatopathies and help clinicians improve the diagnosis and treatment of this condition in humans and in veterinary practice.

Keywords: Liver, Protein Malnutrition, Mice, Stereology

Introduction

Protein-energy malnutrition (PEM) is a major form of malnutrition and is defined as an imbalance between food intake (protein and energy) and the amount that the body requires to ensure optimal growth and function [1, 2]. PEM can cause delays in body maturation as well as affect neurological and musculoskeletal system development [3].

To some extent all tissues can be affected by a hypoproteinic state and the most protein-deficiency affected tissues are those which possess a high cellular turnover [4]. In the liver, protein malnutrition leads to altered liver biochemical characteristics and histology [5, 6]. For instance, consumption of a protein-free diet (PFD) for 5 days changes the mouse liver proteome [7, 8]. The mitochondrial DNA content of the liver is reduced in foetal and early postnatal malnourished rats even when proper nutrition was supplied after weaning [9].

Despite the progress reported so far, knowledge of the mechanisms and pathogenesis of hepatocellular injuries of eating disorders is incomplete [5] and little is known as to the quantitative effects of a hypoproteinic diet on the 3D structure of hepatocytes and whether those effects could be reversed by reunitrition with a normoproteic diet.

Hence, in this study we aimed at investigating the putative effects of a low-protein diet on the 3D structure of hepatocytes in mice using design-based stereology and whether this scenario could be reversed by restoring the adequate levels of protein in the diet. Awareness of these data will add to our better morphological understanding of malnutrition-induced hepatopathies and help clinicians improve the diagnosis and treatment of this condition in humans and in veterinary practice.

Materials and Methods

Animals

This study was approved by the Animal Care Committee of the School of Veterinary Medicine and Animal Science of the University of São Paulo (Reference: 1521/2008). Livers were removed from each of 20 two-month-old male Swiss mice obtained from the Department of Clinical and Toxicological Analyses Animal Facility of the Faculty of Pharmaceutical Sciences of the University of São Paulo

(USP) in Brazil. The animals were housed individually in metabolic cages under similar environmental conditions, with a 12-hour light-dark cycle, temperature of 22±2°C and relative humidity of 55±10% and all subjects fasted for 6 hours and were supplied with water *ad libitum.* After acclimatization for 10 days to the diet [prepared in our laboratory, stored at -4°C until being administered and modified from the American Institute of Nutrition Recommendations for the Adult Rodent (AIN-93M)] [10, 11] the mice were systematically and randomly divided into two main diet groups: n = 10 mice receiving a normoproteinic diet (12% casein/energy) for 5 weeks and n = 10 mice receiving a hypoproteinic diet (2% casein/energy) also for 5 weeks. The full compositions of the diets used in this study are represented in table 1.

When the experiment commenced, all animals (n=20) were 70 days old and the mean (standard deviation) body weight was 41g (1.9g). After 5 weeks, of all animals fed with a normoproteinic diet, 5 were euthanised and used as a control for the undernourished group (CU) at the age of 105 days while 5 were kept alive and received the same diet for five more weeks – as control for the renourished group (CR) at the age of 140 days. Similarly, of all mice fed with a hypoproteinic diet, 5 were euthanised to represent the undernourished group (U) whereas the remaining 5 mice now received a normoproteinic diet for five more weeks – this is the renourished group (R). During the experiment, body weight and feed consumption were evaluated every 48 hours. The denutrition protocol used here was similar to that published by one of the co-authors of this paper [11].

Biochemical tests

On day 105 for the U and CU groups and on day 140 for the R and CR groups, animals were anaesthetised with a combination of 120 $mg.kg^{-1}$ i.m. ketamine chloride and 16 $mg.kg^{-1}$ i.m. xylazine hydrochloride and blood samples were obtained via brachial artery. Animals fasted for 6 hours before blood collection.

Total protein, albumin, globulin, alanine aminotransferase (ALT), alkaline phosphatase (ALP), gamma-glutamyl transpeptidase (GGT), aspartate aminotransferase (AST) and glucose plasma concentrations were measured with the Glucoquant® assay (Roche® Diagnostics GmbH, Mannheim, Germany) [12, 13].

Euthanasia and histology

At specific group-related timepoints (day 105 or 140) animals were euthanised with an i.p. 100 mg.kg^{-1} overdose of sodium pentobarbital (Bayer®). In all animals, a bulbed cannula was inserted into the left ventricle of the heart and a cleansing solution of 0.1 M, pH 7.4 phosphate-buffered saline (PBS, Sigma®) containing 2% heparin (Roche®) and 0.1% sodium nitrite (Sigma®) was injected via the ascending aorta and a perfusion-fixation with 4% formaldehyde and 0.2% glutaraldehyde in PBS (0.1 M, pH 7.4) was conducted using a digital peristaltic perfusion pump with flux control of 6ml/min. Subsequently, the abdominal cavity was incised by a midline incision (celiotomy) and the liver was identified, removed, weighed (wet weight) and immersed in the same fixative solution for 72 hrs at 4^{o}C.

In order to produce vertical and uniform random (VUR) sections [14, 15] livers were rotated along a vertical axis – normal to the organ – and embedded in a 10% agar solution, and exhaustively sectioned with a nominal thickness of 40µm using a VT1000S Leica® vibratome. Next, sections were collected onto glass slides, stained with Mayer's Haematoxylin (Merck®) and mounted under a coverslip with a drop of DPX (Fluka®). Section images were acquired using a DMR Leica microscope equipped with a High-End DP 72 Olympus® digital camera (using either x40 or x63 oil lenses) and projected onto a computer monitor. Stereological analyses were performed using the newCAST Visiopharm® stereology system version 4.4.4.0 (Visiopharm, Copenhagen, Denmark).

Liver volume, V_{LIV}

The total volume of the liver was estimated by means of the Cavalieri principle [16] in the same reference sections used for disectors. Briefly, liver agar-embedded blocks were exhaustively serially sectioned and every 12th section was sampled and measured for cross-sectional area. Then,

$$V_{LIV} := T \cdot \sum A_{LIV},$$

where T is the between-section distance (480 µm) and $\sum A_{LIV}$ is the sum of the delineated profile areas of the chosen set of liver sections. Profile areas were estimated from the numbers of randomly-positioned test points (~300 per liver) hitting the whole reference space and the areal equivalent of a test point.

Shrinkage estimation

Liver fragments were then dissected out, weighed and their wet weights were converted into volumes using a tissue density of 1.06g.cm^{-3} for estimating tissue distortion (shrinkage). Tissue density had been previously estimated in a pilot study – with mice treated with similar conditions – by simply weighing livers and dividing their wet weights (g) (after perfusion-fixation) by their volumes (cm^3) estimated by liquid displacement [17]. Mean tissue densities and their coefficients of variation (CVs) in the groups were 1.059 g/cm^3 (0.10) (CU group), 1.061 g/cm^3 (0.09) (U group), 1.060 g/cm^3 (0.10) (R group) and 1.059 g/cm^3 (0.10) (CR group). Since inter-group differences did not attain significance (p= 0.44), the same tissue density, i.e. 1.06 g/cm^3 was used for all study groups for estimating tissue shrinkage.

The mean volume shrinkage (coefficient of variation, CV, expressed as a decimal fraction of the mean) was estimated to be 3.8% (0.20) in the U group, 3.4% (0.22) in the CU group, 3.1% (0.21) in the R group and 3.9% (0.18) in the CR group. No correction for global shrinkage was performed since between-group differences were not significant (p=0.231).

Total number of hepatocytes: N_{HEP}

The optical fractionator was used for estimating the total number of uninucleate and binucleate hepatocytes (N_{HEP}) [16, 18]. Each liver agar-embedded block was exhaustively serially sectioned into 40 μm-thick sections and a mean sampling fraction (ssf) – 1/28 for CU; 1/36 for U; 1/47 for R and 1/33 for CR groups – of these sections was selected. Before starting the counting procedure, a z-axis distribution was performed in order to: (i) determine the hepatocyte distribution throughout section thickness; (ii) determine the Mayer's Haematoxylin-hepatocyte staining penetration throughout section thickness and (iii) establish the disector height, which was 19 μm for CU and U, and 15 μm for R and CR groups. Section thickness was measured in every field of view using the central point of the unbiased counting frame.

In order to avoid putative bias in the differentiation between uninucleate and binucleate hepatocytes attributed to a non-uniform penetration of Mayer's Haematoxylin staining, it was always checked in every field of view that Mayer's

Haematoxylin staining penetration would be at least 30μm from the uppermost section plane. Therefore, we worked with upper and lower guard zones of 5 μm and 16-20μm respectively.

The mean height sampling fraction (hsf) was 1/2 and the entirely hepatocyte was defined as the counting unit, irrespective of its nuclei number (Fig. 1).

A mean area sampling fraction (asf) of 1/504 of the chosen liver sections was sampled using 2D unbiased counting frames [19] with a frame area equivalent to 5,074 μm^2. In the control for the undernourished group 86 disectors were applied to count 420 hepatocytes ($\sum Q^-$). In the undernourished group an average of 97 disectors were used to count 432 hepatocytes. In the renourished group, 94 disectors were applied to count 625 hepatocytes. Finally, in the control for the renourished group 96 disectors were applied to count 596 hepatocytes.

The total number of hepatocytes was then estimated by multiplying the counted number of particles ($\sum Q^-$) – sampled using disectors – by the reciprocal of the above-stated sampling fractions:

$$N_{HEP} := ssf^{-1} \cdot hsf^{-1} \cdot asf^{-1} \cdot \Sigma Q^-$$

Hepatocyte volume: $\bar{v}_{N\ HEP}$

The mean volume of hepatocytes was estimated by the planar rotator method [20], which is a local and direct estimator of particle volume and uses the disector as a sampling probe. In our study the planar rotator was computer assisted using the 6 half-line rotator probe available in the newCAST Visiopharm stereology system (version 4.4.4.0.) and in the same reference sections used for total number estimation. (Fig. 1.)

Statistical analyses

The precision of a stereological estimate was expressed as a coefficient of error (CE) calculated as described elsewhere [21]. In the Results section, the whole data were expressed as group mean (observed coefficient of variation, CV_{obs}) where CV_{obs} represents standard deviation/mean. Group differences were assessed by either one-way ANOVA or Mood's Median Test using Minitab version 17. When using one-way ANOVA and in the event of significant between-group differences ($p<0.05$) Tukey's Test for multiple comparisons was applied.

Results

Clinical Examination

General symptoms of malnutrition were present in the undernourished mice, e.g. skin folds, mucosa opacity and body weight loss. In addition, edema and fluid accumulation were seen in serous cavities

Food, Protein Consumption and Body Weight

Although the U group had a higher diet consumption when compared to the CU group, this increase did not lead to a rise in protein consumption – in fact the consumption of this nutrient was lower in the U group. (Fig. 2.) In the R group the consumption of diet and protein resumed to normal values and was higher than in the CR group. In relative terms the consumption of protein per unit of body weight (g/g of body weight) was: 0.012 (0.10) in the CU group; 0.003 (0.15) in the U group; 0.012 (0.19) in the R group and 0.014 (0.13) in the CR group. With the exception of mice from the U group ($p = 0.01$) mice from all other three groups (CU, R and CR) had the same consumption of protein per unit of body weight (g/g of body weight).

At the end of the experiment the body weight of the animals of the U group was reduced by 23% when compared to their initial body weight. Conversely, the body weight of animals of the CU group increased by 20%. Finally, mice from the R group presented an increase of about 70% when compared to their body at the beginning of the nutritional rehabilitation, while mice from CR group presented an increase of about 40% in relation to their initial body weight. Body weight variation for CU, U and CR groups was calculated considering mice body weight at the beginning of the denutrition protocol. Body weight variation for the R group was however calculated considering mice body weight at the beginning of the nutritional recovery protocol, i.e. the body weight animals presented after five weeks consuming a hypoproteinic diet. (Fig. 2.)

Biochemical tests

Total protein, albumin, globulin, alanine aminotransferase (ALT), alkaline phosphatase (ALP), gamma-glutamyl transpeptidase (GGT), aspartate aminotransferase (AST) and glucose plasma concentrations are summarised in table 2. There were significant changes in the glucose, alkaline phosphatase, albumin and total protein levels. (Tab. 2.)

Liver volume: V_{LIV}

The stereological data were collated in form of a table (Tab. 3). The volume of the liver amounted to 3,302 mm^3 (0.05) in the CU group, 1,141 mm^3 (0.06) in the U group, 2,870 mm^3 (0.06) in the R group and 3,925 mm^3 (0.05) in the CR group. Apparent inter-group differences were significant (p=0.0001), i.e. each group presented noticeable differences from the others (Fig. 3) (Tab. 3). The precision of liver volume estimation (expressed as CE (V_{LIV})) was 0.015 in the CU group, 0.017 in the U group, 0.012 in the R group and 0.0102 in the CR group.

In addition liver weights were 3.5 g (0.06) in the CU group, 1.21 g (0.05) in the U group, 3.04 g (0.06) in the R group and 4.16 g (0.05) in the CR group. Apparent inter-group differences were significant. (p=0.001.) In relative terms the liver weight per unit of body weight (g/g of body weight) was: 0.040 (0.12) in the CU group; 0.041 (0.15) in the U group; 0.047 (0.12) in the R group and 0.045 (0.13) in the CR group. In mice from all four groups liver weights represented the same proportion per unit of body weight (p = 0.338).

Total number of hepatocytes: N_{HEPuni} and N_{HEPbi}

The total number of uninucleate hepatocytes was 11,874,280 (0.07) for the CU group, 15,988,560 (0.08) for the U group, 29,600,520 (0.13) for the R group and 19,995,200 (0.20) for the CR group. The R group data were different from all remaining groups (p=0.015) (Tab. 3). The precision of number of uninucleate hepatocytes estimation (expressed as CE (N_{HEPuni})) was 0.02 for the CU group, 0.03 for the U group, 0.03 for the R group and 0.04 for the CR group.

The total number of binucleate hepatocytes was 1,549,393 (0.14) for the CU group, 2,941,353 (0.21) for the U group, 3,070,816 (0.20) for the R group and 1,536,403 (0.23) for the CR group. Data from the U and R groups were different from those of CU and CR groups (p=0.005) (Tab. 3). The precision of number of binucleate hepatocytes estimation (expressed as CE (N_{HEPbi})) was 0.03 for the CU group, 0.05 for the U group, 0.03 for the R group and 0.02 for the CR group.

Hepatocyte volume: $\bar{v}_{N\ HEP}$

The mean volume of hepatocytes was 8,223 μm^3 (0.07) for the CU group, 4,475 μm^3 (0.05) for the U group, 8,011 μm^3 (0.02) for the R group and 10,003 μm^3 (0.05) for the CR group. The mean hepatocyte volume provided here is an average value

between uninucleate and binucleate hepatocytes' volumes. Data from the U group or from the CR group were different from all remaining groups (p=0.001) (Tab. 3) (Fig. 4).

Discussion

Biochemical markers of liver function

In the undernourished group the hypoproteinic diet led to an important reduction in albumin (20%) - the concentration of albumin is an excellent gauge of liver protein synthesis [22, 23] and marker of nutritional status [24, 25].

Another important finding was the 291% increase in the alkaline phosphatase (ALP) concentration in the undernourished group. ALP is an enzyme that transports metabolites across cell membranes and is present on the surface of bile duct epithelia. Cholestasis and the accumulation of bile salts enhance the synthesis and release of ALP from the cell surface. ALP levels usually rise late in bile duct obstruction and drop slowly after resolution [22, 26]. We hypothesise that protein malnutrition (2% casein) may have damaged the structure of intra-hepatic biliary ductal system augmenting the concentration of ALP, which was reversed when a normoproteinic diet (12% casein) was reinstated to the animals.

Since the minimum daily amounts of all nutrients (but protein) were ingested by the animals in the malnourished group, we can conclude that the changes observed in our experimental model are mainly the result of the reduction in protein and energy intake compared to the control group.

Liver stereology

In this study design-based stereology was used to monitor the effects of a hypoproteinic diet on the structure of mice liver and determine whether those effects could be reversed by refeeding the animals with a normoproteinic diet.

The most startling finding of this study was just how damaging protein malnutrition is: there was a 65% decrease in the liver volume accompanied by a 46% reduction in the hepatocyte volume and a 90% increase in the total number of binucleate hepatocytes. The hypoproteinic diet (2% casein) in this study led to a severe organ and cell atrophy, i.e. both liver and hepatocytes were reduced to about half their initial size.

Before we started this experiment we had hypothesised that protein refeeding would reverse the above-mentioned deleterious effects on the structure of the liver and yet this proved to be partially correct: the normoproteinic diet (12% casein) was effective in restoring the volume of hepatocytes but failed, nonetheless, to completely reverse the liver atrophy characterised by the reduction of the liver volume. (For more details see below Liver and Hepatocyte volume.) The active participation of the connective tissue in liver diseases - such as cirrhosis - is well established [27] and although we have not measured this structural component of the liver, it is possible that a reduction in the liver connective tissue could be one of a plethora of other factors contributing to the organ atrophy observed in our study. Other factors potentially involved in liver atrophy are discussed below. (see Liver and Hepatocyte volume section.)

Total number of hepatocytes

Methodological considerations

In this study the entirely hepatocyte was defined as the counting unit, irrespective of its nuclei number. When perusing the relevant literature it is possible to learn that authors have mainly used four different stereological approaches to count hepatocytes hitherto: (i) using the nuclei as the counting unit and therefore estimating the total number of hepatocyte nuclei and yet not providing the total number of hepatocytes [28]; (ii) using the nuclei as the counting unit, estimating the numerical density of uni and binucleate hepatocytes and then multiplying these data (numerical density of hepatocyte nuclei) by the liver volume [29]. We argue that this approach would suggest that the authors assumed that the number of hepatocyte nuclei equals the total number of hepatocytes themselves and, if so, we would not agree with this approach; (iii) using the nuclei as the counting unit and discriminating between uni and binucleate hepatocytes in 5 μm-thick physical sections taking into account a correction based upon the mean nucleus height of hepatocytes which again assumes that the distribution of hepatocytes' nuclei heights is the same in the whole liver [30] or (iv) using the aid of immunohistochemistry techniques, i.e. using polyclonal antibodies against carcinoembryonic antigen (CEA) and, because biliary canaliculi are then marked, the authors advocate that an 'unequivocal'

counting of uninucleate and binucleate hepatocytes was achieved [31]. Although we welcome the association between immunohistochemistry and stereology, CEA is not a specific labelling for hepatocytes and yet it is directed against biliary canaliculi as even mentioned in [31] and primarily useful for the study of hepatoblastomas [32]. Therefore, we postulate that an 'unequivocal' identification of uni and binucleate hepatocytes would have not been accomplished solely based upon the use of CEA.

Therefore, we can identify advantages and disadvantages in every technique - including ours - and of course we always aim at producing an accurate and precise estimation of parameters with a lower and acceptable coefficient of error, which we think it was attained in our study. (Please see Total Number of Hepatocytes: N_{HEP} in Materials and Methods section.) In addition we think that it was important the association of perfusion-fixation achieved by a using a digital peristaltic perfusion pump with flux control of 6ml/min with the generation of vertical and uniform random (VUR) sections - the former was important in leading towards an workable tissue fixation, whereas the latter was important to elicit a more uniform penetration of Mayer's Haematoxylin-hepatocyte staining. Indeed, as with [33] Mayer's Haematoxylin-hepatocyte staining was highly appropriate for the identification of hepatocytes since it allowed for a clearly-distinguishable cell membrane against the background of the histological section.

Ultimately, the use of immunohistochemistry was not necessary to render a reliable identification and counting of uninucleate and binucleate hepatocytes, which was always pursued by the same experienced person. (author: Gomes SP.)

Our estimates for the total number of uninucleate hepatocytes in the mice liver are 99% lower than that reported for the rat liver [31] – who have also employed the optical disector – and [34] who elicited their data by means of the physical disector. The mice used in our study were 85% lighter than the rats investigated in [31] who actually demonstrated a positive correlation between animal body weight and the number of binucleate hepatocytes. Using the optical disector the total number of hepatocyte nuclei was estimated in bulb-c mice to be 5.3×10^8 [28]. Unfortunately, the aforementioned authors [28] did not report on the total number

of hepatocytes, which would have allowed for a direct comparison with our data in the same species, i.e. mice.

In our study, although there was a 90% increase in the total number of binucleate hepatocytes and protein malnutrition exerted no effects on the total number of uninucleate hepatocytes. Conversely, protein refeeding indeed led to an 85% increase in the total number of uninucleate hepatocytes. The proportion of binucleate to uninucleate hepatocytes was 13% in the control for the undernourished group; increased to 18% in the undernourished group – explained by the 90% increase in the number of binucleate hepatocytes; subsequently reduced to 10.4% in the renourished group explained by the 85% increase in the number of uninucleate hepatocytes; and finally reached 7.7% in the control for the renourished group. Similarly, very recently, it has been demonstrated that the administration of a proteinic parenteral solution of hepatotrophic factors in partially-hepatectomised rats led to a 44.9% rise in the hepatocyte proliferation rate increasing the liver regenerative capacity [35].

Although we have not used cell proliferation markers such as Ki-67, we have robust 3D design-based stereology-conducted estimations to believe that the 90% increase in the total number of binucleate hepatocytes in the undernourished group (U) do represent hepatocellular proliferation and the latter could be explained by the fact that those cells play an important role in hyperplastic liver reaction (liver plasticity), acting as a cell reservoir for rapid liver regeneration [36, 37] and producing uninucleate hepatocytes through an amitotic cytokinesis [38].

An increase in the proportion of uninucleate hepatocytes generally follows a decrease in the percentage of binucleate hepatocytes – this has been constantly reported in response to dimethylaminobenzene [37] and iethylnitrosamine/phenobarbitone [39] induced hepatocarcinogenesis. By contrast, in the undernourished group the total number of binucleate hepatocytes in fact rose by 90% due to protein malnutrition and yet this was not accompanied by an increase in the total number of uninucleate hepatocytes as seen in [38]. Despite all hypotheses already published in the literature, the functional role of binucleation in hepatocytes, which starts before 3 weeks of post-natal life (day 14),

412 is still unclear, complex and has a multifactorial onset. Just in 2016, micro RNAs
413 (miR-122) have been involved in triggering hepatocyte binucleation in mice [40].

414 **Liver and Hepatocyte volume**

415 Liver and hepatocyte volumes were estimated in bulb-c mice [28]. Bulb-c mice
416 hepatocytes were 55% smaller than those of the Swiss mice we used and their
417 livers are 2-fold smaller. With regards to the hypoproteinic diet used in our study,
418 this led to a 65% decrease in the liver volume accompanied by a 46% reduction in
419 the hepatocyte volume, i.e. organ and cell atrophy respectively.

420 We hypothesise that the 65% reduction in the liver volume of undernourished
421 mice could be mainly caused by the 46% reduction in hepatocyte volume triggered
422 by a lower protein availability in the diet and its induced damage to the hepatocyte
423 structure – other liver structural units such as the biliferous and vascular system
424 could also be reduced and play an additional role in liver atrophy, though we have
425 not measured them. Along similar lines, Parra et al. [41] have shown a 27.4%
426 reduction in liver mass in rats subject to protein-energy malnutrition which was
427 attributed to two factors: (i) decrease in hepatocyte number (hypoplasia) – which
428 has not been confirmed by our data – and (ii) reduction in the size of hepatocytes
429 (atrophy) – the latter has also been shown in our study. According to [41, 42] liver
430 and hepatocyte atrophy was caused by the reduction in the flow of hepatotrophic
431 factors (such as insulin) to the liver after prolonged lack of food ingestion.

432 It is also interesting to observe the dynamic relationships between the liver and
433 its compartment-units. For instance, if the liver size is reduced by 65% in the
434 undernourished mice, how could the organ accommodate simultaneously a 90%
435 increase in the total number of binucleate hepatocytes? The answer may lay on the
436 fact that there was a 46% reduction of cell size (hepatocyte volume), i.e. we could
437 be observing here a compensatory regenerative mechanism related to liver
438 plasticity characterised by a high proliferation rate of smaller binucleate
439 hepatocytes which are now allocated in a smaller (atrophied) organ. Similary,
440 when one compares the control for the renourished with the control for the
441 undernourished group the liver volume of the former is 19% bigger than the latter.
442 This change occurred in conjunction with a 22% increase in the hepatocyte volume
443 (cell hypertrophy) in the control for the renourished group. Therefore, we suggest

that hepatocyte hypertrophy could be one of the main causes of liver hypertrophy seen in this group and yet we cannot rule out that other structural components of the liver such as vascular and biliferous systems as well as the connective tissue could also be implicated in this structural change.

In addition, the liver volume of the renourished group is only 13% lighter than the liver of the control for the undernourished group. Since our renutrition protocol with a normoproteinic diet lasted for five weeks, we strongly believe that liver volume would have been restored to normal values – had the renutrition protocol been expanded for at least one more week – as it was the case for hepatocyte volume, which was restored to normal values after five weeks refeeding subjects with a normoproteinic diet.

Concluding Remarks and Future Research Directions

We believe this study adds to the understanding of protein malnutrition-induced damage to the liver structure. Subsequent lines of research enquiry would be the investigation into the molecular mechanisms governing hepatocyte size recovery and the possible role played by binuclate hepatocytes during protein-refeeding-induced liver regeneration. We also hope that the results elicited by our study can be translated into improving the dietary conditions for populations worldwide, especially for those individuals living in poor and developing countries.

Acknowledgments and Financial Support

This study was supported by São Paulo Research Foundation (FAPESP) and Conselho Nacional de Desenvolvimento Cientifico e Tecnologico. (CNPq.) (Application: 141901/2007-1.)

Conflict of Interest

None.

References

[1] Fock RA, Rogero MM, Vinolo MA, et al. Effects of protein–energy malnutrition on NF-kappaB signalling in murine peritoneal macrophages. Inflammation 2010; 33:101–109.

[2] Bossola M. (2015) Nutritional interventions in head and neck cancer patients undergoing chemoradiotherapy: a narrative review. Nutrients 2015; 7: 265-276.

476 [3] Mayneris-Perxachs J, Bolick DT, Leng J, Medlock GL, Kolling GL, Papin JA,
477 Swann JR, Guerrant RL. Protein- and zinc-deficient diets modulate the murine
478 microbiome and metabolic phenotype. AJCN 2016; 104: 1253-1262.

[4] Deo MG. Biology of protein-calorie malnutrition. Wld Rev Nutr Diet 1978; 32: 49-95.

[5] Caballero VJ, Mendieta JR, Lombardo D, et al. Liver damage and caspase-dependent apoptosis is related to protein malnutrition in mice: effect of methionine. Acta Histochem 2015; 117: 126-35.

[6] Feres NH, Reis SR, Veloso RV et al. Soybean diet alters the insulin- signaling pathway in the liver of rats recovering from early-life malnutrition. Nutrition 2010; 26: 441-448.

479 [7] Sanllorenti PM, Rosenfeld J, Ronchi VP, et al. Two dimensional non
480 equilibrium pH gel electrophoresis mapping of cytosolic protein changes
481 caused by dietary protein depletion in mouse liver. Mol Cell Biochem 2001;
482 220: 49–56.

483 [8] Ronchi VP, Giudici AM, Mendieta JR, et al. Oxidative stress in mouse liver
484 caused by dietary amino acid deprivation: protective effect of methionine. J
485 Physiol Biochem 2010; 66: 93–103.

486 [9] Park KS, Kim SK, Kim MS, et al. Fetal and Early Postnatal Protein Malnutrition
487 Cause Long-Term Changes in Rat Liver and Muscle Mitochondria. The Journal
488 of Nutrition 2003; 133: 3085–3090.

489 [10] Reeves PG, Nielsen FH, Fahey GC Jr. AIN-93 purified diets for laboratory
490 rodents: final report of the American Institute of Nutrition ad hoc writing
491 committee on the reformulation of the AIN-76A rodent diet. J Nutr. 1993;
492 123: 1939-51.

493 [11] Borelli P, Fock RA, Blatt S, et al. Effect of protein deprivation on erytropoiesis.
494 British Journal of Nutrition 2007; 97: 307-314.

495 [12] Kratzsch J, Bier H, Klemm R, et al. Radioimmunoassay for the determination
496 of serum cortiscoterone in ducks (Anas platyrhynchos). Archiv Für
497 Experimentelle Veterinärmedizin 1986; 40: 531-540.

498 [13] Seidel B, Bigl M, Franke H, et al. Expression of purinergic receptors in the
499 hypothalamus of the rat is modified by reduced food availability. Brain
500 Research 2006; 1089: 143-152.

501 [14] Baddeley AJ, Gundersen HJG, Cruz-Orive LM. Estimation of surface area from
502 Vertical Sections. Journal of Microscopy 1986; 142: 259–276.

[15] Kissmeyer-Nielsen P, Christensen H, Laurberg S. Diverting colostomy induces mucosal and muscular atrophy in rat distal colon. Gut 1994; 35: 1275-81.

[16] Gundersen HJ, Bagger P, Bendtsen T, et al. The new stereological tools: disector, fractionator, nucleator and point sampled intercepts and their use in pathological research and diagnosis. Acta Pathologica, Microbiologica et Immunologica Scandinavica 1988; 96: 858-881.

[17] Scherle W A simple method for volumetry of organs in quantitative stereology. Mikroskopie 1970; 26: 57-60.

[18] Gundersen HJ. The smooth fractionator. Journal of Microscopy 2002; 207: 191-210.

[19] Gundersen HJG. Notes of the estimation of the numerical density of arbitrary profiles: the edge effect. Journal of Microscopy 1977; 111: 219-223.

[20] Vedel-Jensen EB, Gundersen HJG. The Rotator. Journal of Microscopy 1993; 170: 35-44.

[21] Gundersen HJG, Jensen EBV, Kieu K, et al. The efficiency of systematic sampling in stereology - reconsidered. Journal of Microscopy 1999; 193: 199–211.

[22] Giannini EG, Testa R, Savarino V. Liver enzyme alteration: a guide for clinicians. Canadian Medical Association Journal 2005; 172: 367-79.

[23] Scheig R. Evaluation of tests used to screen patients with liver disorders. Primary Care 1996; 23: 551-60.

[24] Koyama A, Hashimoto M, Tanaka H, et al. Malnutrition in Alzheimer's Disease, Dementia with Lewy Bodies, and Frontotemporal Lobar Degeneration: Comparison using serumAlbumin, TotalProtein,and Hemoglob in Level. PLoS One. 2016; 11: e0157053. doi: 10.1371/journal.pone.0157053. eCollection 2016.

[25] Neloska L, Damevska K, Nikolchev A, et al. The Association between Malnutrition and Pressure Ulcers in Elderly in Long-Term Care Facility. Open Access Maced J Med Sci. 2016; 4: 423-427.

[26] Schlaeger R, Haux D, Kattermann R. Studies on the mechanism of the increase in serum alkaline phosphatase activity in cholestasis: significance of the hepatic bile acid concentration for the leakage of alkaline phosphatase from rat liver. Enzyme 1982; 28: 3-13.

[27] Youssef WI, Tavill AS. Connective tissue diseases and the liver. Journal of Clinical Gastroenterol 2002; 35: 345-349.

[28] Karbalay-Doust S, Noorafshan A Stereological study of the effects of nandrolone decanoate on the mouse liver. Micron 2009; 40: 471-475.

[29] Neves RH, Alencar AC, Aguila MB, et al. Hepatic stereology of Schistosomiasis mansoni infected-mice fed a high-fat diet. Mem Inst Oswaldo Cruz 2006; 101: 253-60.

[30] Altunkaynak BC, Ozbek E. Overweight and structural alterations of the liver in female rats fed a high-fat diet: A stereological and histological study. Turkish Journal of Gastroenterology 2009; 20: 93-103.

[31] Marcos R, Monteiro RAF, Rocha E. Design-based stereological estimation of hepatocyte number, by combining the smooth optical fractionator and immunocytochemistry with anti-carcinoembryonic antigen polyclonal antibodies. Liver International 2006; 26: 116 -124.

[32] Fasano M, Theise ND, Nalesnik M, et al. Immunohistochemical evaluation of hepatoblastomas with use of the hepatocyte-specific marker, hepatocyte paraffin 1, and the polyclonal anti-carcinoembryonic antigen. Mod Pathol 1998; 11: 934-938.

[33] Luna LG. Manual of Histologic Staining Methods of the Armed Forces Institute of Pathology. 3rd edition. New York: McGraw Hill Publishers, 1968.

[34] Carthew P, Edwards RE, Nolan BM. New approaches to the quantitation of hypertrophy and hyperplasia in hepatomegaly. Toxicology Letters 1998; 102-103: 411-415.

[35] Trotta MR, Cajaiba DM, Parra OM, et al. Parenteral solution of nutritional hepatotrophic factors improves regeneration in thioacetamide-induced cirrhotic livers after partial hepatectomy. Toxicol Pathol 2014; 42: 414-421.

[36] Gandillet A, Alexandre E, Holl V, et al. Hepatocyte ploidy in the normal rat. Comp Biochem Physiol A 2003; 134: 665–673.

[37] Styles JA. Studies on the hyperplastic responsiveness of binucleated hepatocytes. Carcinogenesis 1990; 11: 1149–1152.

[38] Styles JA, Kelly M, Elcombe CR. A cytological comparison between regeneration, hyperplasia and early neoplasia in the rat liver. Carcinogenesis 1987; 8: 391–399.

[39] Jack EM, Bentley P, Bieri F, et al. Increase in hepatocyte and nuclear volume and decrease in the population of binucleated cells in preneoplastic foci of rat liver: a stereolocal study using the nucleator method. Hepatology 1990; 11: 286–297.

[40] Hsu S, Delgado ER, Otero PA, et al. MicroRNA-122 regulates polyploidization in the murine liver. Hepatology 2016; 64: 599-615.

[41] Parra OM, Hernandez-Blazquez FH, De Sousa e Silva RAP, et al. Reduction of liver mass due to malnutrition in rats. Correlation with emaciation of animals and size of organs not inserted in the portal system. Sao Paulo Med J 1995; 113: 903-909.

[42] Starzl TE, Porter KA, Putnam CW. Intraportal insulin protects from the liver injury of portacaval shunt in dogs. Lancet 1975; 2: 1241-1242.

Legend of figures 1-4

Fig. 1. Images of successive focal planes throughout a Mayer's Haematoxylin-stained optical section of a mice liver from the renourished group illustrating the application of the optical disector. The distance between each focal plane is 4 μm. On plane A (uppermost surface of the section) a field of view – selected using an unbiased counting frame – is followed along the whole section thickness (planes B, C, D, E and F) and hepatocytes are sampled and counted as they come into focus on each focal plane. For instance, on plane C (8 μm apart from plane A) two uni (U) and three binucleate (B) hepatocytes are sampled. The uninucleate hepatocyte in the upper left corner of the unbiased counting frame is not sampled since its cell membrane touches the exclusion line. The lowermost focal plane (F) (bottom surface of the section) is 20 μm apart from plane A and no particles are sampled on it. Scale bars: 30 μm.

Fig. 2. Mean diet consumption (grams/day/animal) (A), mean protein consumption (grams/day/animal) (B) and animal body weight range (%) in the experimental groups (C). The number of animals studied in the control for the undernourished (CU), undernourished (U), renourished (R) and control for the renourished (CR) groups is represented by N. $^{*}p \leq 0.05$; $^{***}p \leq 0.005$

Fig. 3. Macroscopic images of the mice liver from the control for the undernourished (CU), undernourished (U), renourished (R) and control for the renourished (CR) groups depicting startling differences in their sizes, i.e. protein-deficient diet led to a serious liver atrophy - 65% reduction in liver volume of undernourished animals - which was not reversed with protein refeeding. Scale bar: 2 cm

Fig. 4. Light-microscopic images of Mayer's Haematoxylin-stained optical sections of a mice liver from the control for the undernourished (A), undernourished (B), renourished (C) and control for the renourished (D) groups depicting details of the liver microstructure. Protein-deficient diet led to a serious hepatocyte atrophy - 46% reduction in the cell volume (B) - which was reversed with protein refeeding (R). Scale bars: 30 μm.

Table 1.

Full composition of the normoproteinic and hypoproteinic diets administered to the mice used in this study

Ingredients	**Normoproteinic diet (g/Kg diet)**[a]	**Hypoproteinic diet (g/Kg diet)**[a]
Casein (>85%)[b]	120	20
Sucrose	100	100
Fiber	50	50
Soybean oil	40	40
Mineral mix[c]	35	35
Vitamin mix[d]	10	10
L-cystin	1.8	0.3
Choline bitartrate	2.5	2.5
Cornstarch	640.7	742.2
Tert-butylhydroquinone	0.008	0.008

[a] Both diets were prepared in our laboratory and their composition was according to AIN-93M rodent diet.

[b] Casein supplied by Labsynth® (Brazil).

[c] Mineral mix supplied by Rhoster Indústria e Comércio LTDA (Brazil) (mineral mix for AIN-93M rodent diet).

[d] Vitamin mix supplied by Rhoster Indústria e Comércio LTDA (Brazil) (vitamin mix for AIN-93M rodent diet).

Table 2. Biochemical parameters in mice from control for the undernourished (CU), undernourished (U), renourished (R) and control for the renourished (CR) groups. Values are group means (CVs).

Biochemical parameters	Groups			
	CU	U	R	CR
Total protein (g/dL) *	5.4^{A} (0.05)	5.18^{B} (0.11)	5.96^{A} (0.07)	5.92^{A} (0.03)
Albumin (g/dL) **	2.18^{A} (0.04)	1.75^{B} (0.06)	2.12^{A} (0.05)	2.2^{A} (0.02)
Globulin (g/dL) ^{NS1}	2.4^{A} (0.07)	2.1^{A} (0.20)	2.2^{A} (0.09)	2.23^{A} (0.07)
Alanine aminotransferase (U/L) ^{NS2}	44.3^{A} (0.30)	9.0^{A} (0.30)	13.33^{A} (0.25)	41^{A} (0.32)
Alkaline phosphatase (U/L) ***	106^{A} (0.11)	414^{B} (0.38)	147.7^{A} (0.17)	$159.3^{A,B}$ (0.04)
Gamma-glutamyl transpeptidase (U/L) ^{NS3}	0.33^{A} (0.17)	1.33^{A} (0.11)	0.22^{A} (0.12)	0.22^{A} (0.12)
Aspartate aminotransferase (U/L) ^{NS4}	105.3^{A} (0.38)	135^{A} (0.37)	100^{A} (0.21)	126.3^{A} (0.16)
Glucose (mg/dL) ****	178^{A} (0.19)	76.7^{B} (0.20)	117^{A} (0.29)	156^{A} (0.07)

Means that share the same letter (A or B) are not significantly different (^{NS}).
$^{NS1}p = 0.60$; $^{NS2}p = 0.074$; $^{NS3}p = 0.227$; $^{NS4}p = 0.591$

Means that do not share the same letter (A or B) are significantly different (*).
$^{*}p = 0.03$; $^{**}p = 0.02$; $^{***}p = 0.021$; $^{****}p = 0.02$

Table 3. Stereological parameters in mice from control for the undernourished (CU), undernourished (U), renourished (R) and control for the renourished (CR) groups. Values are group means (CVs).

Stereological parameters	Groups			
	CU	U	R	CR
Liver volume (mm^3) *	3,302^{A} (0.05)	1,141^{B} (0.06)	2,870^{C} (0.06)	3,925^{D} (0.05)
Total number of uninucleate hepatocytes**	11,874,280^{A} (0.07)	15,988,560^{A} (0.08)	29,600,520^{B} (0.13)	19,995,200^{A} (0.20)
Total number of binucleate hepatocytes***	1,549,393 ^{A} (0.14)	2,941,353 ^{B} (0.21)	3,070,816^{B} (0.20)	1,536,403 ^{A} (0.23)
Hepatocyte volume (μm^3) ****	8,223^{A} (0.07)	4,475^{B} (0.05)	8,011^{A} (0.02)	10,003^{C} (0.05)

Means that do not share the same letter (A, B, C or D) are significantly different (*).
*p = 0.0001; **p = 0.015; ***p = 0.005 **** p = 0.001

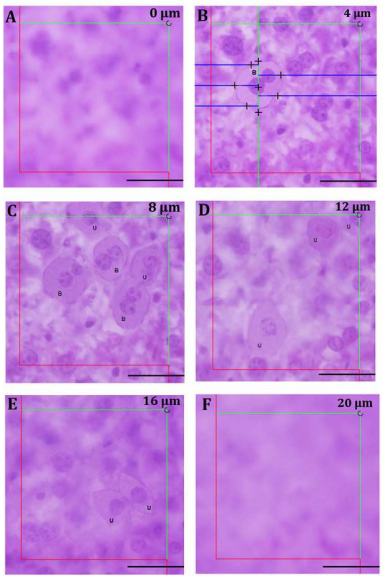

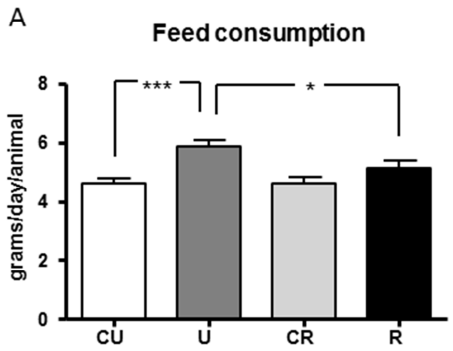

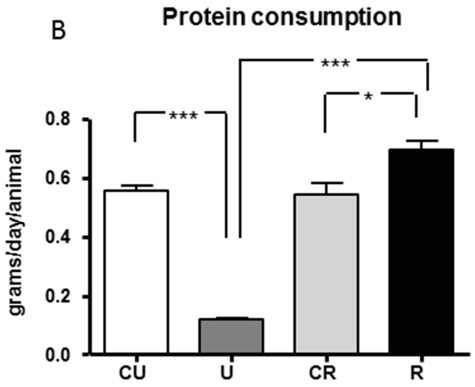

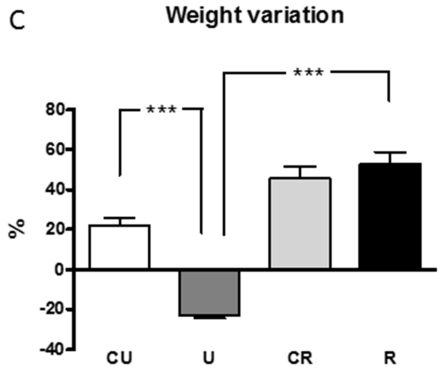

N:
CU=5
U=5
CR=5
R=5

$^{*}p \leq 0.05$; $^{***}p \leq 0.005$

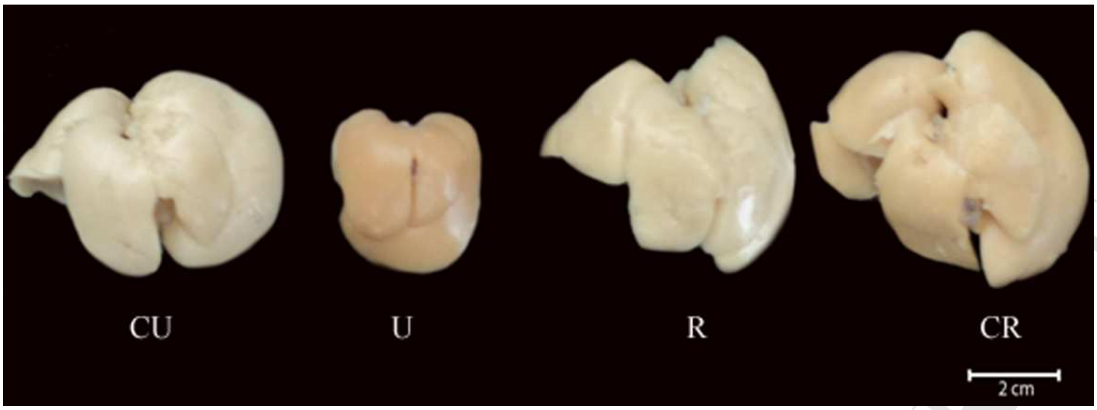

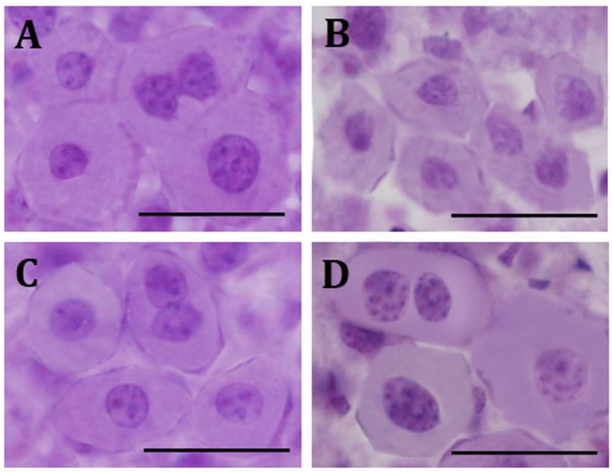

HIGHLIGHTS

- This is a study about the 3D structure of the mice liver which shows - using 3D Quantitative Microscopy technology - that protein malnutrition (2% casein in the diet) induced a 65% decrease in the liver volume;

- Accompanied by a 46% reduction in the hepatocyte volume and a 90% increase in the total number of binucleate hepatocytes, which indicates proliferative capacity activating liver plasticity;

- After renutrition - reinstating a normoproteinic diet (12% casein) – it proved to be effective in restoring the size of hepatocytes, led to an 85% increase in the total number of uninucleate hepatocytes and partially reversed liver atrophy (liver volume reduction).